(Received 10 May 2025, Accepted 17 June 2025, Scheduled 29 June 2025)

High-Performance Compact Antenna for Sub-6 GHz 5G MIMO Applications

Rajendran Dhananjeyan[1, *], Mohit Pant[2], Kumarasamy Vishalatchi[3], Subramaniyan Janarthanan[4], Ponnusamy Sukumar[5], Dhanushkodi Siva Sundhara Raja[6], and Dhandapani Rajesh Kumar[7]

[1] *SRM Valliammai Engineering College, India*
[2] *Mahakal Institute of Technology, India*
[3] *AAA College of Engineering and Technology, India*
[4] *Sethu Institute of Technology, India*
[5] *Nandha Engineering College, India*
[6] *SACS MAVMM Engineering College, India*
[7] *Vel Tech Rangarajan Dr. Sagunthala R & D Institute of Science and Technology, India*

ABSTRACT: This study presents a compact four-port antenna optimized for sub-6 GHz 5G MIMO systems. The design incorporates a crescent-shaped radiating element paired with a defected ground structure (DGS) to improve both bandwidth and port-to-port isolation. Operating within the 3.2–3.8 GHz frequency band, the antenna maintains a VSWR below 2. The orthogonal arrangement of the radiators effectively suppresses mutual coupling, ensuring that isolation levels exceed −15 dB. Simulated and measured results validate the design, demonstrating a maximum gain of 5 dBi and radiation efficiency reaching up to 80%. Key MIMO performance indicators — such as envelope correlation coefficient (ECC), total active reflection coefficient (TARC), channel capacity loss (CCL), and diversity gain (DG) — confirm the antenna's suitability for robust 5G communication.

1. INTRODUCTION

Recent advancements in 5G antenna technologies between 2023 and 2025 have focused on improving performance, miniaturization, flexibility, and integration to support enhanced mobile broadband, ultra-reliable low-latency communications, and massive machine-type communications. In the sub-6 GHz range, metasurface-based 4T4R multiple-input multiple-output (MIMO) antennas have been proposed for vehicle-to-everything and internet of things (IoT) applications, achieving high gain and wide bandwidth with good isolation characteristics [1]. A compact 2-port MIMO antenna with rectangular patches and ground plane slots has shown high isolation and low envelope correlation coefficients (ECC < 0.01) across 3.0–4.0 GHz, making it suitable for mid-band 5G applications [2]. For mmWave bands, a flexible quasi-Yagi-Uda antenna operating at 28 GHz has demonstrated stable end-fire radiation and mechanical robustness under bending, paving the way for wearable mmWave 5G devices [4]. A four-port MIMO antenna using defected ground structures achieved excellent performance over 26.8–29.3 GHz with more than 2.5 GHz bandwidth, isolation better than −35 dB, and gain exceeding 18 dBi [5]. Graphene-based flexible antennas have also been explored for 5G wearable systems due to their light weight, conductivity, and resilience, especially for applications like head imaging and body-centric networks [5]. Reconfigurable wearable antennas using nematic liquid crystals have shown tunability in the 3.3–3.8 GHz band with ultra-low power control (< 2.5 V), ideal for integration into smart glasses and adaptive wearable platforms [6, 7]. Shared-aperture antenna designs have also gained interest for supporting both sub-6 GHz and mmWave operation in a single structure, effectively reducing footprint while supporting multi-band communication [8]. Qualcomm introduced miniaturized mmWave antenna modules with a 25% reduction in volume, optimized for smartphones and AR/VR systems, without sacrificing beamforming capability [9]. Complementing this, iCana launched a 28 GHz beamforming integrated circuit (IC) capable of 800 MHz bandwidth and advanced signal path control for dense phased arrays [10]. The rise of MIMO has emphasized the need for beam management; new studies addressed the importance of codebook design and feedback algorithms to support large antenna arrays with minimal complexity [11–13]. Furthermore, hybrid beamforming arrays with dynamic phase-shifter control are implemented to improve spectrum reuse and link reliability in urban scenarios [14, 15]. Metamaterial-based reconfigurable antennas have also emerged, offering frequency agility and beam steering while maintaining compactness, which is critical for vehicular and drone-based 5G networks [16]. Reviews have emphasized how combining dielectric resonator antennas (DRAs) with planar feeding structures enhances bandwidth and thermal stability at mmWave bands, enabling efficient integration into high-density platforms [17]. The challenges of high mutual coupling and narrow bandwidths in small form factors are addressed using electromagnetic bandgap (EBG) structures and defected ground planes, which enhance isolation

* Corresponding author: Rajendran Dhananjeyan (dhananj13@gmail.com).

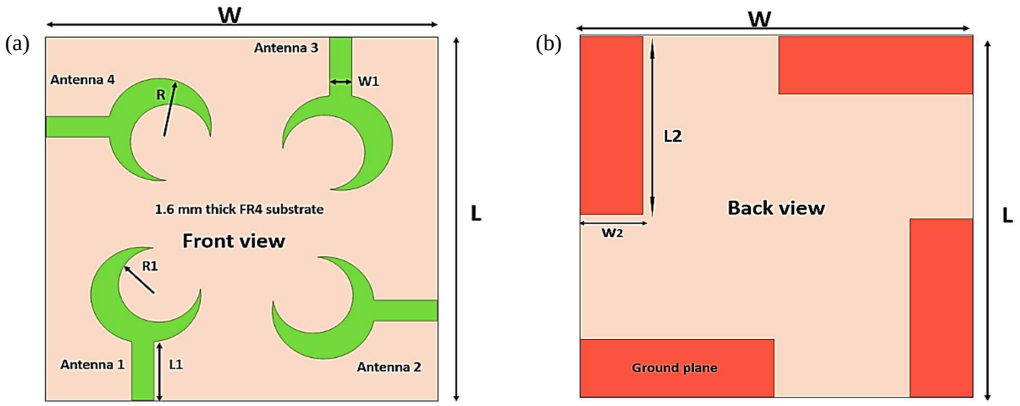

FIGURE 1. Layout of the proposed crescent-shaped four-port antenna: (a) Front view, (b) rear view.

and impedance matching [18, 19]. In terms of system-level integration, recent design strategies now include co-packaged radio frequency (RF) front ends and antennas, reducing path losses and enhancing energy efficiency in 5G access points [20]. Finally, comprehensive reviews have cataloged the diverse range of approaches adopted across academia and industry, summarizing the key breakthroughs in materials, geometry optimization, and integration strategies for 5G and beyond [21]. Collectively, these developments signify a shift toward high-performance, compact, and multifunctional antennas that can seamlessly operate across sub-6 GHz and mmWave frequencies, while also adapting to the form-factor constraints and environmental variability of future wireless ecosystems.

The research gap identified in literature revolves around the lack of compact, multi-element MIMO antenna designs tailored for sub-6 GHz 5G applications, especially with an emphasis on achieving high isolation and low envelope correlation coefficient (ECC) in small form factors. Many existing studies either focus on two-port MIMO antennas or large systems, while few explore compact four-port MIMO solutions with high isolation and low mutual coupling. Additionally, while simulation results are common, there is a scarcity of designs validated through both simulation and experimental measurements, alongside comprehensive MIMO performance analysis using key metrics like ECC, TARC, CCL, and DG. This work addresses this gap by presenting a compact four-element MIMO antenna designed specifically for sub-6 GHz 5G, featuring a crescent-shaped radiating patch and a defective ground structure. This design ensures high isolation, low ECC, and a peak gain of 5 dBi, with both simulated and measured results demonstrating its reliability and suitability for modern 5G MIMO applications.

The antenna design and analysis began with carefully selecting substrate material and geometric configuration to achieve compactness and wideband performance. Following the initial design, a detailed parametric analysis was conducted to evaluate the influence of key parameters such as substrate height, patch dimensions, and slot geometry on antenna performance. To gain deeper insight into the radiation mechanism, the surface current distribution was examined at the resonant frequencies, highlighting the active regions responsible for radiation and coupling. Subsequently, the fabricated prototype was tested, and the measured results were discussed in comparison with the simulated data, showing good agreement in terms of impedance bandwidth and return loss. The antenna's gain and efficiency were analyzed across the operating frequency range, revealing stable and satisfactory performance suitable for wireless communication applications. Finally, in the context of multiple-input multiple-output (MIMO) systems, key MIMO parameters such as envelope correlation coefficient (ECC), diversity gain, and isolation between antenna elements were evaluated, confirming the design's suitability for modern high-data-rate communication systems.

2. ANTENNA CONFIGURATION AND DESIGN ANALYSIS

Figure 1 presents the structural layout of the proposed four-port MIMO antenna. The design is implemented on an FR4 substrate with a thickness of 1.6 mm and an overall footprint of 60 mm $\times$ 60 mm. Each of the four crescent-shaped radiators is symmetrically positioned at the corners on the front side. These radiators are defined using arcs with radii $R = 8$ mm and $R1 = 6$ mm to create the crescent geometry. The feeding lines are designed with dimensions $W1 = 2$ mm and $L1 = 8$ mm to ensure proper impedance matching. The radiating elements are oriented orthogonally to minimize mutual coupling and improve isolation — key requirements for MIMO systems. On the rear side, a defective ground structure (DGS) is implemented using partial ground patches with dimensions $W2 = 4$ mm and $L2 = 14$ mm. This ground modification interrupts surface current flow, enhancing both bandwidth and isolation. This combined front-back configuration is optimized to deliver reliable operation across the target 3.2–3.8 GHz band, offering stable radiation patterns and efficient signal propagation.

Figures 2(a) and 2(b) illustrate the simulated reflection and transmission coefficients of the antenna system. The reflection coefficient plots confirm impedance matching within the 3.2–3.8 GHz band, with return losses below -10 dB. Transmission coefficients between elements remain better than -15 dB throughout the operating band, signifying low mutual coupling.

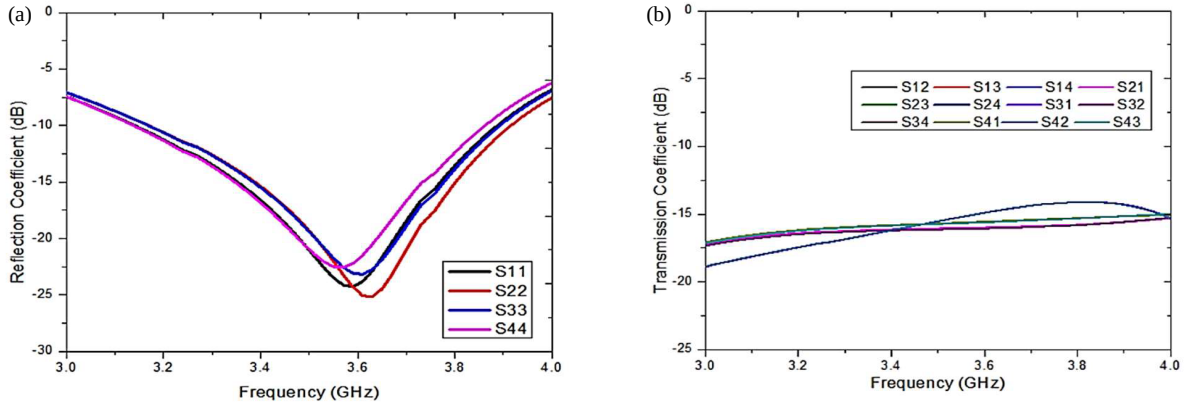

FIGURE 2. Simulated results: (a) Reflection coefficients, (b) transmission coefficients.

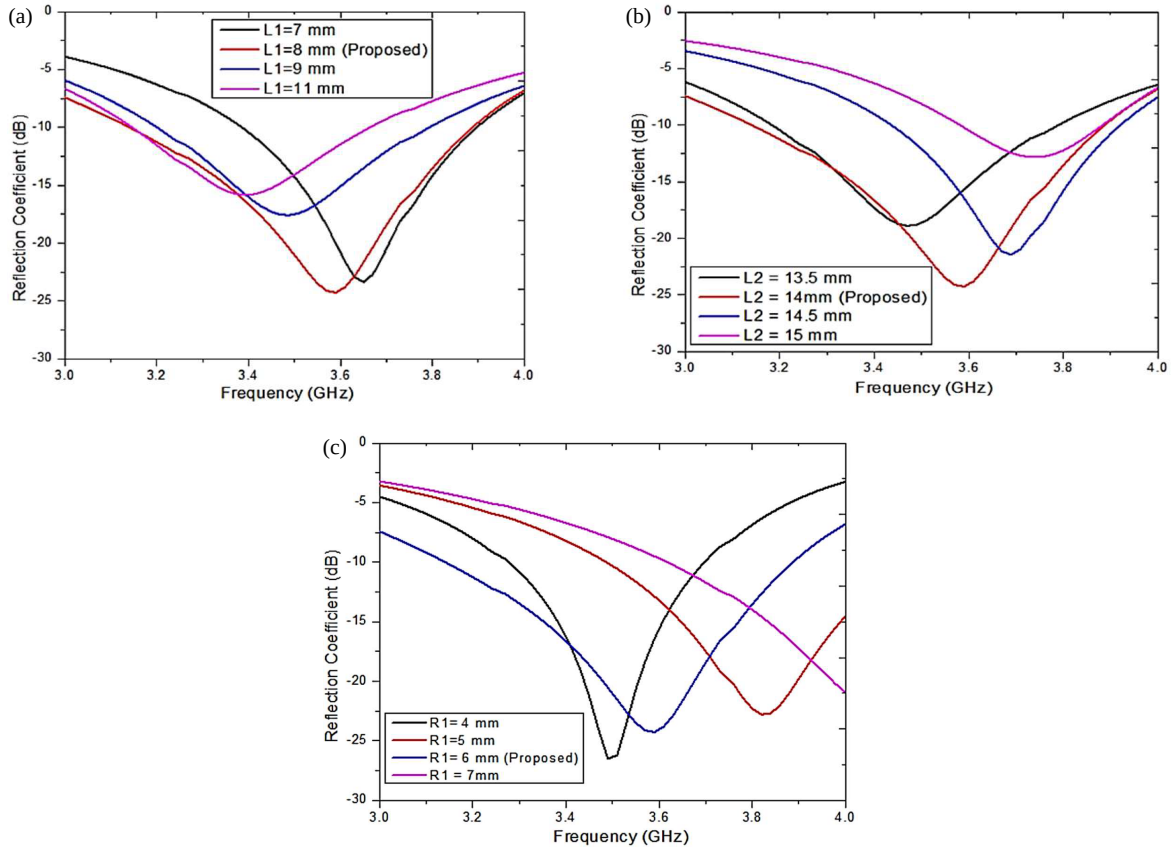

FIGURE 3. Parametric studies of (a) feed line length $L1$, (b) ground length $L2$, (c) inner radius $R1$.

2.1. Parametric Study

Figures 3(a)–5(c) explore the impact of key parameters on antenna performance. Adjusting the feed line length ($L1$) from 6.9 mm to 10.9 mm shifts the resonance leftward, with 7.9 mm identified as the optimal length. Modifying ground length ($L2$) from 13.5 mm to 15 mm affects impedance matching, with 14 mm providing the best response. Altering the inner radius ($R1$) from 4 mm to 7 mm expands the operational bandwidth.

2.2. Surface Current Distribution

Figure 4 displays the current distribution at 3.5 GHz when port 1 is excited. Concentrated current is observed near the feed and crescent curve, with minimal coupling to the other elements, supporting the antenna's low mutual coupling performance.

3. MEASURED RESULTS AND DISCUSSIONS

The fabricated prototype and its measurement setup are depicted in Figure 5.

Figure 6(a) displays the reflection coefficients (S_{11}, S_{22}, S_{33}, and S_{44}) for a four-element antenna, spanning from 3 GHz to 4 GHz. At approximately 3.6 GHz, the reflection coefficients for all four ports drop to around -25 dB, indicating minimal signal reflection and excellent impedance matching. Beyond 3.7 GHz and below 3.6 GHz, the reflection coefficients

TABLE 1. Performance comparison of the proposed work with existing work.

Reference	[3]	[7]	[12]	[14]	[19]	Proposed work
Antenna size (mm^2)	40×40	80×80	30×30	112×112	40×40	60×60
Frequency (GHz)	2.2–3.5	3.54–3.72 & 5.04–5.16	4.58–6.12	5.15–5.35	4.7–5.1	3.2–3.8
Distance among antenna elements (mm)	8	28	9	NR	16	4.7
Isolation (dB)	-14	-18	-10	-22	-25	-15
Gain (dBi)	3.1	4	4.02	4.8	2.8	5
ECC	< 0.2	< 0.2	< 0.15	< 0.15	< 0.01	< 0.16

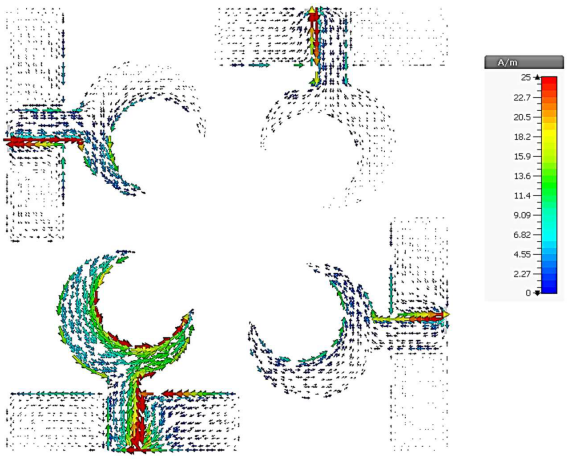

FIGURE 4. Surface current distribution at 3.5 GHz with port 1 active.

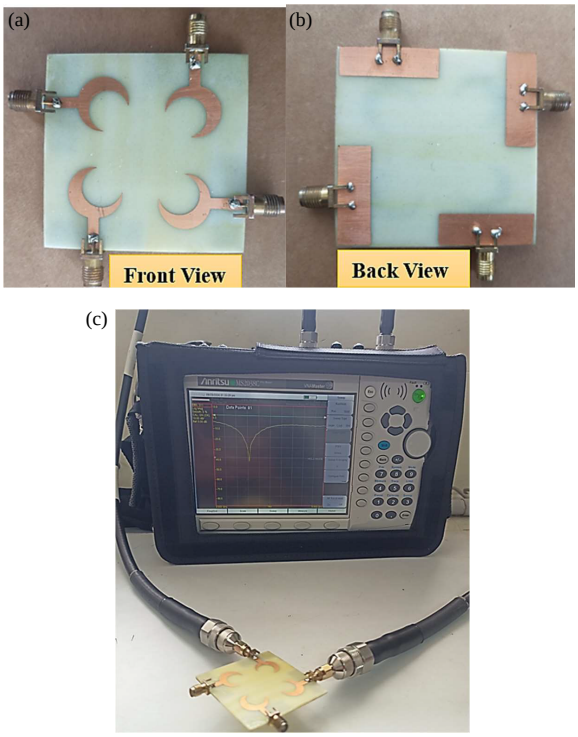

FIGURE 5. Fabricated prototype: (a) Front view, (b) back view, (c) measurement setup.

increase and approach the -10 dB level, indicating reduced efficiency. However, within the shaded frequency range of 3.2 GHz to 3.8 GHz, the antenna demonstrates reliable performance for multi-port applications. All ports exhibit good impedance matching, with reflection coefficients remaining below -10 dB. Figure 6(b) displays the S-parameters, which represent the transmission characteristics between the ports of the multi-port system, across the frequency range of 3.0 GHz to 4.0 GHz. The y-axis, measured in decibels (dB), ranges from -25 dB to 0 dB. Transmission paths, such as S_{12}, S_{21}, and S_{31}, are represented by different colors and symbols. The transmission coefficients remain relatively stable, generally between -15 dB and -17 dB, indicating minimal signal loss. Within the operational band of 3.2 GHz to 3.8 GHz, the transmission remains consistent with only slight variations across all signal paths.

Figures 7(a) and (b) illustrate the measured and simulated E-plane radiation patterns of the proposed antenna, respectively. The results confirm that the antenna exhibits an omnidirectional radiation pattern in the E-plane, with strong agreement between the measured and simulated data.

Figure 8 shows the efficiency response over the frequency range of 3.0–4.0 GHz. Efficiency increases from approximately 60% at 3 GHz to a maximum above 80% near 3.8 GHz, beyond which it slightly declines.

Figure 9 plots the gain response over the same frequency span. The antenna delivers a peak gain of approximately 5 dBi near 3.8 GHz, gradually increasing from 2 dBi at 3 GHz.

4. MIMO PERFORMANCE

Figure 10 provides a comprehensive overview of the antenna system's performance across the 3 GHz to 4 GHz range. The ECC (Envelope Correlation Coefficient) remains low (below 0.16) throughout, especially in the 3.2 GHz to 3.8 GHz range, indicating minimal correlation between antenna signals and optimal MIMO performance. The diversity gain is consistently high around 10 dB across all antenna pairs, confirming reliable signal performance for MIMO applications, with a stable peak within the 3.2 GHz to 3.8 GHz range. TARC (Total Active Reflection Coefficient) decreases with frequency, reaching its minimum at 3.6 GHz, with phase angle having

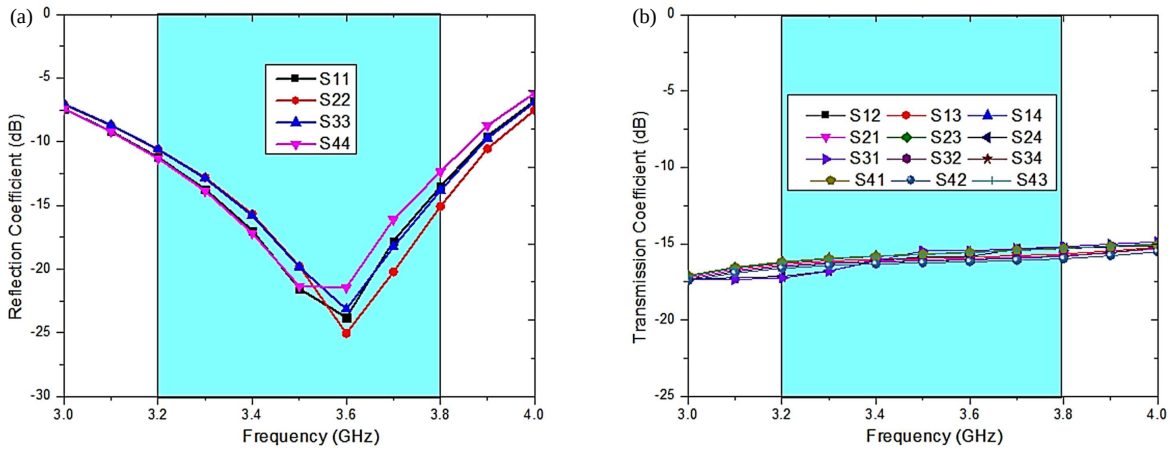

FIGURE 6. Measured S parameters: (a) Reflection co-efficient, (b) transmission co-efficient.

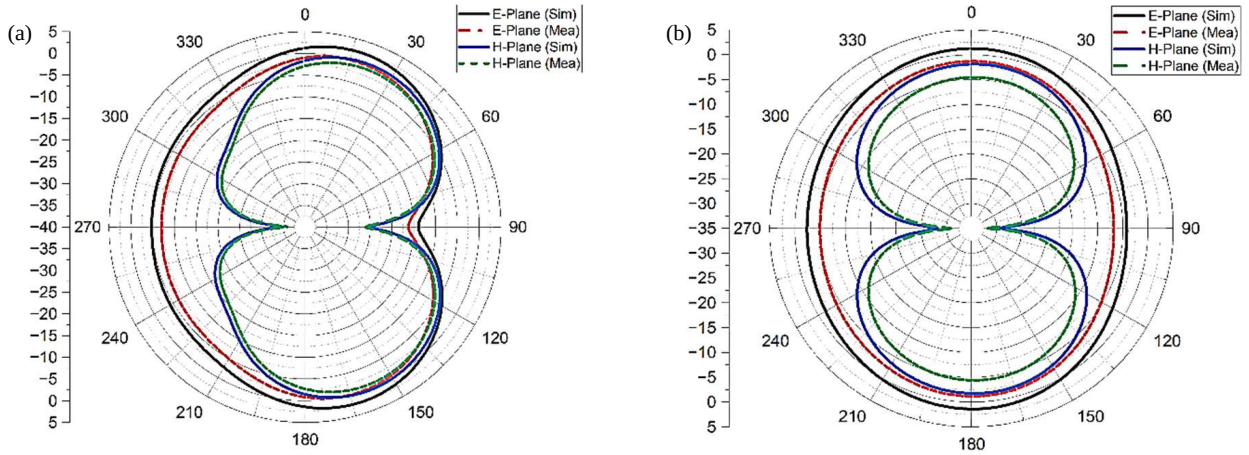

FIGURE 7. Radiation pattern at (a) 3.5 GHz, (b) 3.7 GHz.

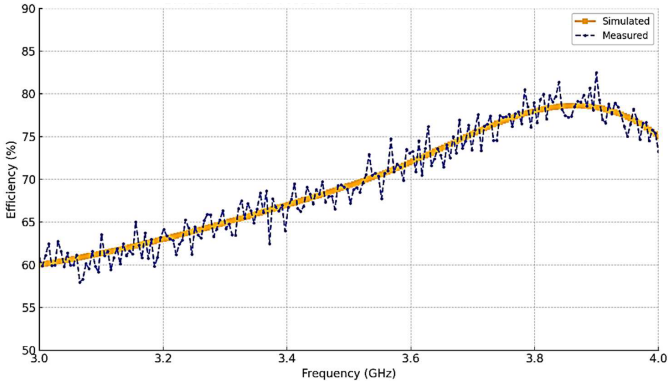

FIGURE 8. Simulated and measured radiation efficiencies of antenna 1.

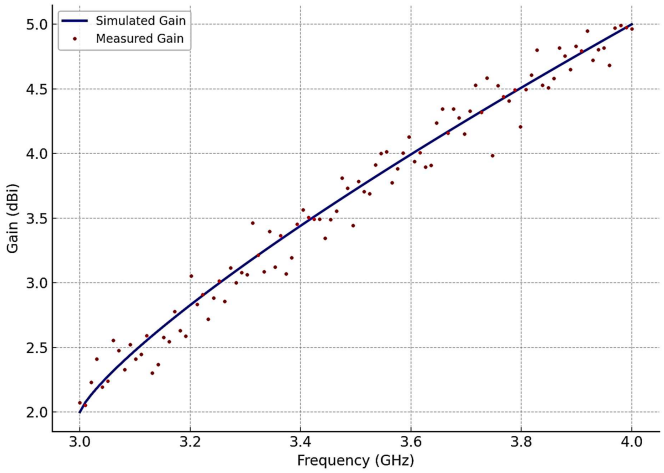

FIGURE 9. Simulated and measured gains of antenna 1.

minimal impact, especially between 3.2 GHz and 3.8 GHz. Lastly, the channel capacity loss is frequency-dependent, staying constant at 0.20 bps/Hz between 3.0 GHz and 3.2 GHz, rising to 0.30 bps/Hz at 3.8 GHz, and slightly decreasing afterward. Overall, the system demonstrates excellent MIMO performance, minimal reflection, and stable channel capacity, particularly in the 3.2 GHz to 3.8 GHz range.

The proposed antenna exhibits a balanced and superior performance compared to the antennas reported in [3, 7, 12, 14, 19] as listed in Table 1. With a compact size of $60 \times 60\,\text{mm}^2$, it maintains a smaller footprint than larger designs such as [7] ($80 \times 80\,\text{mm}^2$) and [14] ($112 \times 112\,\text{mm}^2$), while supporting

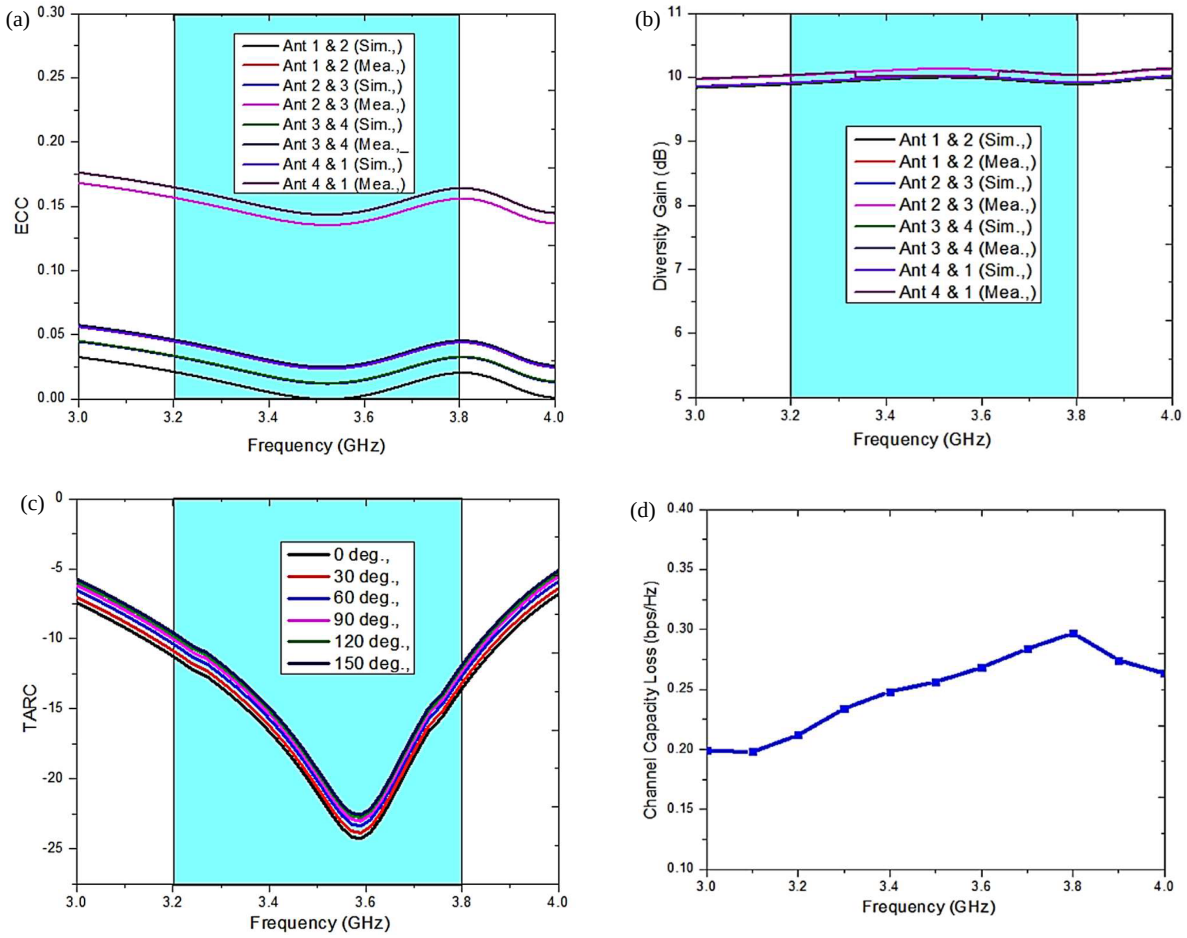

FIGURE 10. MIMO parameters: (a) ECC, (b) diversity gain, (c) TARC, (d) channel capacity loss.

a wider operational bandwidth from 3.2 to 3.8 GHz, which is highly suitable for sub-6 GHz 5G applications. Notably, the proposed antenna achieves the shortest distance between antenna elements (4.7 mm), enabling higher integration density, which is crucial for modern MIMO systems. Despite this close spacing, it maintains good isolation at -15 dB, which is competitive with other designs and superior to that in [3] and [12]. Additionally, it offers the highest gain at 5 dBi, enhancing signal strength and coverage. The envelope correlation coefficient (ECC) remains low at < 0.16, indicating strong MIMO performance, and remains within acceptable limits despite the compact design. Collectively, the proposed antenna outperforms others by offering a compact, high-gain, closely packed MIMO solution with solid isolation and low ECC, ideal for space-constrained, high-performance wireless applications.

5. CONCLUSION

This work presents a compact, high-isolation four-port MIMO antenna specifically engineered for sub-6 GHz 5G applications. The design employs crescent-shaped radiating elements alongside a defected ground structure (DGS) to ensure efficient operation within the 3.2–3.8 GHz frequency range. Radiators are positioned orthogonally to minimize mutual coupling, achieving inter-port isolation levels exceeding -15 dB. The antenna's performance is substantiated through both simulation and experimental measurements, demonstrating strong agreement. It delivers a peak gain of 5 dBi and attains a radiation efficiency of up to 80%. Key MIMO parameters — including envelope correlation coefficient (ECC), total active reflection coefficient (TARC), channel capacity loss (CCL), and diversity gain (DG) — are within desirable thresholds, affirming the antenna's potential for dependable multi-port communication. Featuring a compact form factor of 60 mm $\times$ 60 mm and fabricated on a cost-effective FR4 substrate, the proposed antenna offers a practical solution for portable 5G-enabled devices. Its blend of miniaturization, efficiency, and effective isolation underscores its viability for future wireless systems.

REFERENCES

[1] Guntupalli, K. B. R., V. K. Pandey, and M. A. Ansari, "Compact metasurface MIMO antenna design for 5G V2X applications," *arXiv preprint arXiv:2309.07131*, 2023.

[2] Sahu, S., S. Kumari, and R. Sharma, "Design of 5G MIMO antenna for mobile handsets," *Book Chapter in AERT, STM Journals*, 2023.

[3] Sarkar, D. and K. V. Srivastava, "Compact four-element SRR-loaded dual-band MIMO antenna for WLAN/WiMAX/WiFi/4G-LTE and 5G applications," *Electronics Letters*, Vol. 53, No. 25,

1623–1624, 2017.

[4] Ur Rehman, M., M. A. Imran, Q. H. Abbasi, and A. Alomainy, "Flexible Quasi-Yagi-Uda antenna for wearable 5G applications," *arXiv:2108.13180*, 2023.

[5] Chandra, K., M. Pradhan, and S. N. Sahu, "Millimeter-wave MIMO antenna for IoT-based 5G applications," in *Proceedings of ICACCT 2023*, Banur, India, 2023.

[6] Zulkifli, A. A., M. H. Jamaluddin, R. Yusof, and N. H. Osman, "Graphene-based flexible antennas for head imaging systems," *Micromachines*, Vol. 14, No. 3, 2023.

[7] Dwivedi, A. K., A. Sharma, A. K. Singh, and V. Singh, "Design of dual band four port circularly polarized MIMO DRA for WLAN/WiMAX applications," *Journal of Electromagnetic Waves and Applications*, Vol. 34, No. 15, 1990–2009, 2020.

[8] Nguyen, P. T., M. T. Vu, H. C. Nguyen, T. T. Nguyen, and A. M. Cao, "Tunable flexible wearable antennas using liquid crystals for 5G applications," *arXiv preprint arXiv:2212.08622*, 2023.

[9] Yin, F., Y. Li, Y. Lin, L. Zhang, and Q. Wu, "Review on shared-aperture antennas for 5G/6G systems," *Micromachines*, Vol. 13, No. 5, 2023.

[10] Qualcomm Technologies Inc., "Qualcomm shrinks size of mmWave antenna modules by 25%," *5G Technology World*, 2024.

[11] iCana Corporation,, "Launch of beamforming IC for 5G mmWave applications," *PR Newswire*, Sep. 2023.

[12] Yang, M. and J. Zhou, "A compact pattern diversity MIMO antenna with enhanced bandwidth and high-isolation characteristics for WLAN/5G/WiFi applications," *Microwave and Optical Technology Letters*, Vol. 62, No. 6, 2353–2364, 2020.

[13] Alkhateeb, A., "Massive MIMO for 5G/6G: Beamforming and codebook design," *arXiv preprint arXiv:2301.13390*, 2023.

[14] Das, G., N. K. Sahu, A. Sharma, R. K. Gangwar, and M. S. Sharawi, "FSS-based spatially decoupled back-to-back four-port MIMO DRA with multidirectional pattern diversity," *IEEE Antennas and Wireless Propagation Letters*, Vol. 18, No. 8, 1552–1556, 2019.

[15] Kwon, H., Y. Kim, S. Lee, and J. Choi, "Hybrid beamforming for mmWave MIMO in 5G networks," *IEEE Access*, Vol. 12, 2024.

[16] Kumar, D. S., E. Kalaiarasi, B. E. Caroline, P. Ajitha, A. Sivasangari, and S. Lalithakumari, "Investigation of the patch antenna characteristics with the impact of metamaterial," in *2022 IEEE 2nd International Conference on Mobile Networks and Wireless Communications (ICMNWC)*, 1–4, Tumkur, Karnataka, India, Dec. 2022.

[17] Singh, J. and A. Chandra, "DRA-based mmWave antennas for 5G base stations," *IET Microwaves, Antennas & Propagation*, 2023.

[18] Ahmed, S., S. R. Khan, A. Rahman, and M. T. Islam, "Mutual coupling reduction in 5G MIMO using EBGs and DGS," *Electronics*, Vol. 13, No. 2, 2024.

[19] Ali, H., X.-C. Ren, I. Bari, M. A. Bashir, A. M. Hashmi, M. A. Khan, S. I. Majid, N. Jan, W. U. K. Tareen, and M. R. Anjum, "Four-port MIMO antenna system for 5G n79 band RF devices," *Electronics*, Vol. 11, No. 1, 35, 2022.

[20] Bose, R., A. Shukla, S. Pal, and R. K. Singh, "RF-front-end and antenna co-design for 5G access points," *IEEE Microwave Magazine*, Vol. 25, No. 3, 2025.

[21] Gao, Y., J. Zhang, C. Wang, S. Li, and W. Chen, "Survey on 5G antennas: Design, trends, and challenges," *Micromachines*, Vol. 14, No. 7, 2024.